On a Satellite Coverage Problem

DANNY T. CHI
Kodak Berkeley Research

YU T. SU
National Chiao Tung University

The earth coverage area for a satellite in an Earth synchronous orbit with a non-zero inclination angle is a function of the time of day. Locating the area where an Earth terminal can establish a link with a geosynchronous satellite at a certain period of the day is of great concern to system designers. A special case of much interest is when the time period of satellite coverage is 24 h. Two simple and rapid algorithms for locating 24 h satellite coverage areas are presented. One of the proposed algorithms can also be applied to determine other airborne antenna coverage problems.

I. INTRODUCTION

Because of lunar and solar gravitational attraction, geosynchronous satellite orbits do not remain perfectly circular. They can also be intentionally inclined to provide greater coverage to higher altitudes, even as high as the north and south poles [1]. Of special concern to communication engineers is not only whether a ground terminal has a direct view of the desired satellite, or the other way around, but also whether the communication link can be established, i.e., whether the link power budget renders enough signal power margin at the receiver site. A ground terminal is said to be covered by a geosynchronous satellite if both conditions are met. In the case of inclined orbits, this status of coverage, given the terminal location, is a function of the time of day because the terminal elevation angle, the atmospheric conditions, and the terminal to satellite distance all vary with time.

A 24 h or all-day coverage area (ADCA) is defined as the area within which it is possible, at any time and under specified weather conditions and a fixed terminal altitude, to establish a link with a given geosynchronous satellite. For convenience, we assume that the reference altitude is sea level. The assumptions of a fixed altitude and uniform climate and atmospheric conditions in the ADCA definition are necessary to eliminate the time variation, although a coverage area is very likely to cross different climatic regions and will definitely have altitude variations. Such an ADCA can thus be regarded as the best case (maximum coverage area) or the worst case (minimum coverage area) result, depending on the specific atmospheric parameters and link availability requirement used in the calculation.

Two efficient algorithms for locating ADCAs in the latitude-longitude $(L - L)$ plane are presented. In the next section a relationship between the link budget computation and the satellite coverage is established through a single parameter. The problem of coverage status checking is then simplified to examine an inequality. A few useful properties of ADCAs are derived and then applied to develop an efficient algorithm in Section III. Another algorithm and numerical examples are presented in the following section. This second algorithm uses an observation derived from a simple geometric viewpoint. It can also be extended to evaluate the coverage area in any given time period and for any circular satellite orbit. Section V gives a brief summary of our results and suggests possible extensions.

II. LINK BUDGET AND EARTH COVERAGE AREA

The received carrier-to-noise power ratio $(C/N)_{rec}$ for a one-way ground terminal to satellite link is given

by [2, ch. 4]

$$\left(\frac{C}{N}\right)_{\text{rec}} = \text{EIRP}\left(\frac{\lambda}{4\pi d}\right)^2 L_a L_r \left(\frac{G}{T}\right)\left(\frac{1}{kB}\right) \quad (1)$$

where

EIRP	transmitter effective isotropic radiated power,
λ	carrier wavelength,
d	slant range from satellite to Earth terminal,
L_a	atmospheric and weather loss,
L_r	rain attenuation,
k	Boltzmann constant,
B	noise bandwidth of satellite channel (Hz),
G/T	receiver antenna gain-to-noise temperature ratio.

The atmospheric and rain losses depend on the link availability requirement, the height of the terminal, the carrier frequency, the weather conditions, e.g., rain rate, height of $0°$ C isotherm, mean local surface absolute humidity, mean local surface temperature (see [3] for details), and ϕ, the terminal elevation angle. For fixed altitude, frequency and weather conditions, the total propagation path loss is then a function of the elevation angle only. For example, if ϕ is greater than $6°$, then the atmospheric loss can be approximated by [3, Fig. 6.2-3]

$$L_a(\phi) = K^{\csc(\phi)} \quad (2)$$

where K depends on carrier frequency, ground altitude, mean surface relative humidity, and mean local surface temperature. Under the same assumptions, the rain attenuation statistics is also a function of the elevation angle only; see [3, Fig. 6.3.-1] for an analytic estimation procedure for L_r. An implicit assumption of (1) is that the terminal antenna boresite always points to the satellite antenna boresite. This and the constant terminal altitude assumption imply that there is a one-to-one correspondence between ϕ and θ, the angle between the Earth terminal and the satellite, both viewed from the center of the Earth.[1] Therefore the product $L_r L_a$ will be denoted by $L(\theta)$ henceforth. Note that the carrier-to-noise power ratio calculated by (1) should be interpreted statistically, i.e., on the average, the actual $(C/N)_{\text{rec}}$ will be less than the value so obtained for at most $p\%$ of the year, where p is the designed link outage used in estimating L_r.

If a perfect symmetric satellite antenna pattern is assumed then it can be shown that the received carrier-to-noise ratio of the satellite should satisfy the inequality

$$\left(\frac{C}{N}\right)_{\text{rec}} = \frac{k_0 L(\theta)}{h^2 + 2R_e R_a(1 - \cos\theta)} \geq \left(\frac{C}{N}\right)_{\text{req}} \quad (3)$$

---

[1]This angle is often referred to as the central angle [2].

where $(C/N)_{\text{req}}$ is the required C/N, R_e is the radius of the Earth, h is the height of the satellite above the Earth, R_a is the distance between the satellite and the Earth center, and $k_0 = G/T[\text{EIRP}/(4\pi\lambda)^2](1/kB)$. Therefore if the maximum angle θ_c which satisfies (3) is known, the condition under which an Earth terminal located at (Ψ,ψ) can close a link (for at least $p\%$ of the year) with a satellite whose subsatellite point at time t is (Ψ_t,ψ_t) can be expressed as

$$\cos\psi\cos\Psi\cos\psi_t\cos\Psi_t + \sin\psi\cos\Psi\sin\psi_t\cos\Psi_t$$

$$+ \sin\Psi\sin\Psi_t > \cos\theta_c. \quad (4)$$

In other words, equating both sides of (3) and solving the associated equation using established atmospheric loss and rain attenuation models, we then obtain the maximum angle θ_c that accounts for the combined effect of all the linkage parameters, the required link availability, bit error probability, the assumed weather conditions and terminal altitude on the coverage problem under investigation. For Earth terminal locations with a θ less than θ_c, the associated path loss will be smaller than that for locations whose θ is equal to θ_c, and hence the requirement (3) will be satisfied. The angle θ_c is henceforth referred to as the *coverage angle* and the corresponding spherical circle radius R as the coverage radius; see Fig. 1. For a perfect geostationary satellite at $(\Psi_t,\psi_t) = (0,0)$ for all t, (4) becomes

$$\cos\Psi\cos\psi > \cos\theta_c. \quad (5)$$

It is well known that an inclination of the geostationary orbit will cause the subsatellite point to move in a figure 8 pattern [1, 2]. To decide whether a given (Ψ,ψ) belongs to the ADCA, it is necessary to check whether (4) is satisfied for all subsatellite points (Ψ_t,ψ_t) on the figure 8 pattern.

III. PROPERTIES OF FIGURE 8 PATTERNS AND THE ADCA

The equations governing relative latitude and longitude behavior of the figure 8 pattern for an inclination angle i are given by[2]

$$\bar{\lambda} = \sin^{-1}(\sin i \sin\Phi) \quad (6)$$

$$\bar{\Phi} = \tan^{-1}(\cos i \sin\Phi, \cos\Phi) - \Phi \quad (7)$$

where $\Phi = 2\pi t/T$, $T = 24$ h, $t = $ the normalized time of the day, and the function $\tan^{-1}(x,y)$ is a modified version of the conventional arctangent defined by

$$\tan^{-1}(x,y) = \theta$$

---

[2]A similar set of equations was given in [1, (6-4)], but its second equation indicates an incorrect moving direction. We thus rederive the figure 8 equations in Appendix A.
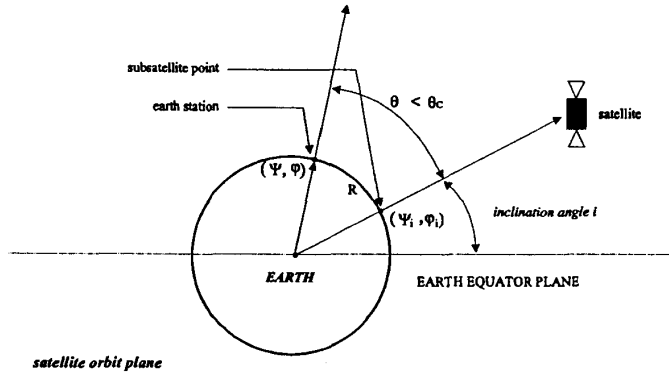
Fig. 1. Inclined geosynchronous satellite with coverage angle θ and coverage radius R.

if and only if

$$\sin\theta = \frac{y}{\sqrt{x^2+y^2}}, \qquad \cos\theta = \frac{x}{\sqrt{x^2+y^2}}, \qquad x^2+y^2 \neq 0.$$

For convenience, it is often assumed that at $t = 0$, the subsatellite point is at $\Phi = 0$, $\lambda = 0$ (see Appendix B). This normalization is used throughout the subsequent discussion. From the above equations, we can easily derive some useful properties of the figure 8 pattern. These properties are summarized below.

PROPERTY 1 *The figure 8 pattern is symmetric with respect to both latitude and longitude axes.*

PROPERTY 2 *The maximum latitude deviation from the equator for the figure 8 pattern is equal to i.*

PROPERTY 3 *The figure 8 equation can be rewritten as* $\bar{\Phi}(\Phi) = \tan^{-1}(\cos i \tan\Phi) - \Phi$, *if* $0 \le t \le 6$, $i > 0$. *The maximum longitude deviation from the ascending node is therefore given by*

$$\sin^{-1}\left(\cot i \sqrt{\frac{1-\cos i}{\cos i}}\right) - \sin^{-1}\left(\frac{\sqrt{1-\cos i}}{\sin i}\right). \quad (8)$$

A brute-force approach to locating the 24 h coverage area would be to check every points in the $L - L$ plane whether the condition (4) is met for all $t \in [0,24)$. Looking for possible reductions in the number of points to be checked, we first observe that Property 1 and (3) lead to the following property.

PROPERTY 4 *The ADCA is symmetric with respect to both latitude and longitude axes.*

Therefore, we need only to search the ADCA in the first quadrant. The second reduction comes from Property 5.

PROPERTY 5 *An upper bound for the intersection of an ADCA with the altitude axis is* $\pm(\theta - i)$, *with the longitude axis intersection* $\pm\cos^{-1}(\cos\theta/\cos i)$.

Note that if $i > \theta$, then the subsatellite point of the ascending node (A in Fig. 2) can be covered either
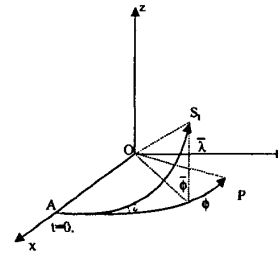

Fig. 2. Subsatellite points of inclined synchronous satellite orbit.

at $t = 6$ or at $t = 18$ only. Its ADCA is thus equal to zero. The third reduction can be accomplished by noting that the coverage area for a fixed satellite (or subsatellite) position is a spherical circular area which is a convex set and that the intersection of convex sets on a sphere is still a convex set. Therefore, we have the following.

PROPERTY 6 *The area of an ADCA is a convex set on the Earth.*

In other words, for each longitude (or latitude) circle we need only two points to determine the portion of the ADCA that belongs to that circle. Another reduction can be derived from the following.

PROPERTY 7 *The latitude of an ADCA boundary in the first quadrant is a decreasing function of longitude.*

The proofs of the above properties are straightforward and are omitted. Taking these properties into account, we can eliminate a large portion of the $L - L$ plane from the search domain and thus an efficient search algorithm for the ADCA such as that described in Fig. 3 can be obtained. However, we still have to deal with the problem of checking the condition imposed by (4) for all t in a certain time period. In other words, the ADCA evaluated by the above algorithm is only a close approximation since we have "quantized" the search domain (see Fig. 3). In the next section, we develop a
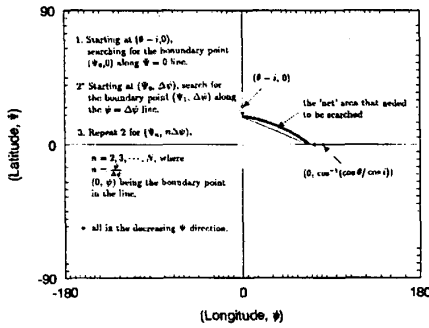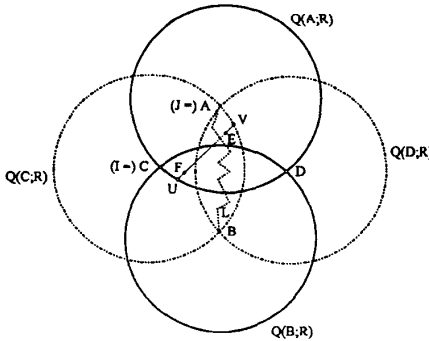
Fig. 3. Coverage area boarder search algorithm.

Fig. 4. Subsatellite point trajectory and coverage area. Note if L is subairplane curve of airplane with constant altitude and antenna coverage radius R, then region $Q(A;R) \cap Q(B;R)$ is always covered by airplane during period when its subairplane point travels through L.

fast algorithm which allows us to check only a finite set of points on the figure 8 pattern.

IV. FAST ALGORITHM FOR LOCATING COVERAGE AREAS

DEFINITION 1   Let A be a point on a sphere S. Then $Q(A;R)$ denotes the spherical circle centered at A with spherical radius R on S.

DEFINITION 2   A curve L joining points A and B on S is said to satisfy the R-condition if and only if L is enclosed by $Q(C;R)$ and $Q(D;R)$, where C and D are points of intersection of $Q(A;R)$ and $Q(B;R)$.

If a curve L (such as a figure 8 pattern) does not satisfy the R-condition, then we can decompose L into a number of subarcs that do satisfy the R-condition. As is seen later, the number of subarcs in a decomposition is proportional to the complexity of the given coverage problem. On the other hand, the decomposition of a given curve is quite straightforward, as the following algorithm demonstrates (Fig. 4).

Let us consider the decomposition of curve $\widehat{AB}$. We can start with the initial point A, select a nearby point P_1 on L, and then check whether the arc $\widehat{AP}_1$

satisfies the R-condition. This test can be done analytically or by checking whether the points $A + j\Delta$, $j = 1,\ldots,n$, $\Delta = AP_1/n$, along the arc $\widehat{AP}_1$ are all within the intersection of $Q(A;R)$ and $Q(B;R)$. If $\widehat{AP}_1$ passes the test, we then choose another point P_2 between P_1 and B on L and perform the test on $\widehat{P_1P_2}$. If it doesn't, we replace P_1 by a point Q_1 between A and P_1 and check whether $\widehat{AQ}_1$ satisfies the R-condition. This process can be repeated until we reach end point B. To reduce the number of subarcs that satisfy the R-condition, we can replace the R-condition by the R'-condition, where R' is slightly larger than R. For example, if $R = 6378$ km (the radius of the Earth), we can replace R by $R(1 + \varepsilon)$, $\varepsilon = 0.0001$. The error introduced by such a substitution is negligible, but the number of subarcs reduced may be significant.

Our second ADCA algorithm is based on the following theorem.

THEOREM.   *Let L be a curve joining points A and B on a sphere S. Suppose L lies within the area $G(C,D;R)$. Then $G(A,B;R)$, the area on S enclosed by $Q(A;R)$ and $Q(B;R)$, is equal to the area $G(L;R)$ enclosed by all spherical circles $Q(p;R)$, where $p \in L$.*

The proof of this theorem is given in Appendix B. As a consequence of this theorem we immediately obtain the following corollary.

COROLLARY.   *Let L be the curve of all the subsatellite points of a satellite in an inclined circular synchronous orbit having a coverage radius R. Suppose L has a decomposition $P_0P_1 \cup \cdots \cup P_{n-1}P_n$ such that each subarc satisfies the R-condition. Then an Earth terminal can establish a communication link with the satellite all the time if and only if the terminal is covered by all $Q(P_j,P)$, $0 < j < n + 1$.*

All the points $P_0,\ldots,P_n$ can be precalculated and therefore the satellite coverage problem is reduced to the task of checking only a finite number of points in a figure 8 pattern. To demonstrate the utility of the fast algorithm, let us consider the case where the angle of inclination i is 5 deg and θ_c, the coverage angles, are 61.8°, 52.5°, 25.7°, and 12.8° (their corresponding terminal antenna elevation angles are 20°, 30°, 60°, and 75°, respectively). The number of points on the figure 8 pattern that need to be checked for each ADCA is listed in Table I. Here we assume that $\Delta = 0.05$ h $= 3$ min and $\varepsilon = 10^{-3}$ (see Section III). The resulting Earth ADCA contours are illustrated in Fig. 5. As mentioned before, we need to search only the first quadrant; therefore, for the case $\theta_c = 61.8°$ only 11 points on the figure 8 pattern (Table I) have to be checked. The ratio of the reduction in the number of points checked is at least $(24/\Delta)/11 = 44.6$. Evidently, this improvement is an increasing function of the required resolution Δ in the fast algorithm.
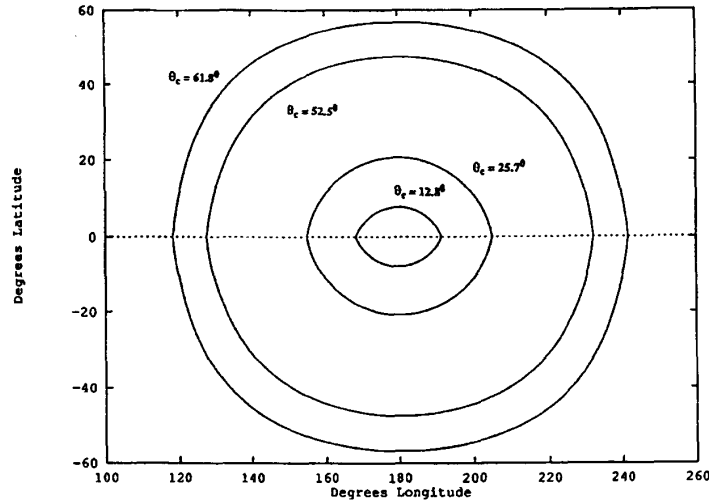
Fig. 5. ADCAs for synchronous satellite with inclined angle 5°.

V. CONCLUSION

In this paper we have derived a general condition for determining the coverage area of a satellite. Two algorithms for determining the continuous coverage area of an inclined circular geosynchronous satellite have been presented. Although we have restricted our discussion to one way (up link) coverage problems only, extensions to simplex or duplex Earth station links are straightforward.

The second algorithm can also be applied to similar airborne coverage problems if 1) the coverage area is a spherical circle, i.e., the antenna pattern is symmetric with respect to its boresite and 2) the aircraft is moving with constant height above the Earth. There is no need to restrict the time period to 24 h, as the first algorithm does. With only minor modifications, it may also be used to predict the coverage area where an Earth station can simultaneously establish links with several satellites in the same orbit. Another application example is illustrated in Fig. 3. Suppose an airplane with coverage radius R wants to monitor the region $Q(A;R) \cap Q(B;R)$. Then the airplane could choose any path as long as its *subairplane* path is within the region $Q(C;R) \cap Q(D;R)$.

APPENDIX A. FIGURE 8 PATTERN OF SUBSATELLITE POINTS

Let T be the period of a satellite orbit and point A be the subsatellite point on the equator; see Fig. 2. Suppose the subsatellite point passes A at time zero. After t hours, the subsatellite point is at point S and A is rotated along the equator to a point P whose coordinate is given by $(x, y, z) = (\cos\Phi, \sin\Phi, 0)$, where $\Phi = \angle AOP = \angle AOS = 2\pi t/T$ and t is the normalized time of day. The coordinates of point S

TABLE I

θ_c	61.8	52.5	25.7	12.8
No. of points	11	15	19	23

can be obtained from P by rotating the x-axis through the angle of the inclination of the satellite i. If the x-axis is rotated through the angle i, the coordinate of S is

$$\begin{bmatrix} 1 & 0 & 0 \\ 0 & \cos i & -\sin i \\ 0 & \sin i & \cos i \end{bmatrix} \begin{bmatrix} \cos\Phi \\ \sin\Phi \\ 0 \end{bmatrix} = \begin{bmatrix} \cos\Phi \\ \cos i \sin\Phi \\ \sin i \sin\Phi \end{bmatrix}. \quad (9)$$

Let Φ and λ be the relative longitude and altitude of S with respect to P; then

$$\cos\Phi = \cos\overline{\lambda}\cos(\Phi + \overline{\Phi}) \quad (10)$$

$$\cos i \sin\Phi = \cos\overline{\lambda}\sin(\Phi + \overline{\Phi}) \quad (11)$$

$$\sin i \sin\Phi = \sin\overline{\lambda} \quad (12)$$

and therefore

$$\overline{\lambda} = \sin^{-1}(\sin i \sin\Phi) \quad (13)$$

$$\overline{\Phi} = \tan^{-1}(\cos i \sin\Phi, \cos\Phi) - \Phi \quad (14)$$

APPENDIX B. PROOF OF THE MAIN THEOREM

Let E and F be two points on a sphere S. Then $\overset{\frown}{EF}$ denotes the (great circle) arc joining E and F and $|EF|$ is the length.

LEMMA. *Let $Q(A;R)$ and $Q(B;R)$ be two spherical circles on a sphere S. Suppose $Q(A;R)$ and $Q(B;R)$ intersect at points C and D on S. Let $G(A,B;R)$ be*

the area on S enclosed by $Q(A;R)$ and $Q(B;R)$ and $G(C,D;R)$ be the area on S enclosed by $Q(C;R)$ and $Q(D;R)$. Then the spherical distance between an arbitrary point in $G(A,B;R)$ and an arbitrary point in $G(C,D;R)$ is less than or equal to R.

PROOF. Let E be an arbitrary point in $G(A,B;R)$ and F be an arbitrary point in $G(C,D;R)$. Suppose $\widehat{EF}$ or its extension intersects the convex set $Q(I;R)$ at a point V, where $I = C$ or D, in the order of $A - V - B$ on $Q(I;R)$ and $\widehat{EF}$ or its extension intersects the convex set $Q(J;R)$ at a point U, where $J = A$ or B, in the order of $C - U - D$ on $Q(J;R)$ (see Fig. 3, where we assume that $J = A$ and $I = C$). It is clear that $\widehat{JU}$ always intersects $\widehat{IV}$ and hence $\widehat{JU}$ is always between $\widehat{JV}$ and $\widehat{JI}$. We now assume that $V \neq J$ and $U \neq I$, otherwise, $|EF| \leq |UV| = R$ and the Lemma is proved.

Notice that in the spherical triangle $\triangle JIV$, $|IV| = |IJ|$, thus $\angle JVI = \angle VJI$ and

$$\angle VJU = \angle VJI - \angle UJI \tag{15}$$

$$\leq \angle VJI + \angle IVU \tag{16}$$

$$= \angle JVI + \angle IVU \tag{17}$$

$$= \angle JVU. \tag{18}$$

Similarly, we observe that in the spherical triangle $\triangle UJV$, $\angle VJU \leq \angle JVU$. Therefore, $\widehat{JU} \leq \widehat{UV}$ and $|EF| \leq |UV| \leq |JU| = R$, and the Lemma is proved.

With this Lemma we now give the proof of the main theorem as follows.

PROOF.

1) $G(A,B;R) \subset G(L;R)$.

Let E be an arbitrary point in $G(A,B:R)$ and p be an arbitrary point on the curve L. L is enclosed by $G(C,D;R)$ and thus $P \in G(C,D;R)$. The above Lemma implies that the spherical distance between P and E is equal to or less than R and E is inside $Q(P;R)$. Therefore, $E \in G(L,R)$ and $G(A,B;R) \subset G(L;R)$.

2) $G(L;R) \subset G(A,B;R)$.

Let E be an arbitrary point in $G(L;R)$. Then E is enclosed by all the spherical circles $Q(P;R)$, where $P \in L$. In particular, E is enclosed by $Q(A;R)$ and $Q(B;R)$. Hence, $G(L;R) \subset G(A,B;R)$.

COROLLARY. *Let L be a curve joining points A and B on a sphere S. Suppose L satisfies the R-condition. Then a point T is enclosed by all $Q(P;R)$, $P \in L$, if and only if T is enclosed by $G(A,B;R)$.*

REFERENCES

[1] Spilker, J. (1977)
       Digital Communications by Satellite.
       Englewood Cliffs, NJ: Prentice-Hall, 1977.

[2] Ha, T. T. (1990)
       Digital Satellite Communications (2nd ed.).
       New York: McGraw-Hill, 1990.

[3] Ippolito, L. J. (1989)
       Propagation Effects Handbook for Satellite System Design
       (4th ed.).
       NASA, 1989.

Danny T. Chi received his Ph.D. in mathematics from University of Southern California, Los Angeles, 1984.

From 1984 to Aug. 1988 he worked at LinCom Corporation, Los Angeles, as a system analyst. In Aug. 1988 he joined Cyclotomics (currently, Kodak Berkeley Research) as a project engineer. He has done research on the Reed-Solomon encoding and decoding algorithms. He has been responsible for a number of projects including Cinema Digital Sound system, NASA's OMV project, Space Station error detection and correction system, and more recently, Kodak's Photo CD project. His research interests are in areas of coding theory, digital signal processing, satellite communications and data compression. He has published numerous papers in these areas.
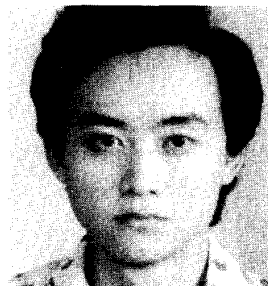
Yu T. Su received the B.S.E.E. degree from Tatung Institute of Technology, Taiwan, in 1974, and the M.S. and Ph.D. degrees in electrical engineering from the University of Southern California, Los Angeles, in 1983.

From 1983 to 1989 he worked at LinCom Corporation, Los Angeles. Since Sept. 1989, he has been a member of the faculty of National Chiao Tung University, Hsinchu, Taiwan, at the MIRC Research Center and the Department of Communication Engineering. His main research interests are in the areas of communication theory and statistical signal processing.